Calhoun

Institutional Archive of the Naval Postgraduate School

Calhoun: The NPS Institutional Archive

Faculty and Researcher Publications	Faculty and Researcher Publications

2009-04-21

Axions as Dark Matter Particles

Duffy, Leanne D.

http://hdl.handle.net/10945/35430

Axions as Dark Matter Particles

Leanne D. Duffy[1] and Karl van Bibber[2]

[1] Los Alamos National Laboratory, Los Alamos, NM 87545, USA
[2] Lawrence Livermore National Laboratory, Livermore, CA 94550, USA and the Naval Postgraduate School, Monterey, CA 93943, USA

E-mail: `lduffy@lanl.gov, kvanbibber@llnl.gov`

Abstract. We review the current status of axions as dark matter. Motivation, models, constraints and experimental searches are outlined. The axion remains an excellent candidate for the dark matter and future experiments, particularly the Axion Dark Matter eXperiment (ADMX), will cover a large fraction of the axion parameter space.

1. Introduction

Despite our knowledge of dark matter's properties, what it consists of is still a mystery. The standard model of particle physics does not contain a particle that qualifies as dark matter. Extensions to the standard model do, however, provide viable particle candidates. The axion, the pseudo-Nambu-Goldstone boson of the Peccei-Quinn solution to the strong CP problem [1, 2, 3, 4], is a strongly motivated particle candidate. We review the strong CP problem and its resulting axion in section 2.

In the early universe, cold axion populations arise from vacuum realignment [5, 6, 7] and string and wall decay [8, 9, 10, 11, 12, 13, 14, 15, 16, 17, 18, 19, 20]. Which mechanisms contribute depends on whether the Peccei-Quinn symmetry breaks before or after inflation. These cold axions were never in thermal equilibrium with the rest of the universe and could provide the missing dark matter. The cosmological production of cold axions is outlined in section 3.

Current constraints on the axion parameter space, from astrophysics, cosmology and experiments, are reviewed in section 4. The signal observed in direct detection experiments depends on the phase-space distribution of dark matter axions. In section 5, we discuss possible structure for dark matter in our galactic halo and touch on the implications for detection. Experimental searches and their current status are discussed in section 6. Finally, the current status of the QCD axion is summarized in section 7.

This is a brief review, designed to overview the current status of axions as dark matter. For more advanced details, we refer the reader to the extensive literature (e.g. reviews can be found in refs. [21, 22, 23, 24, 25]).

2. The strong CP problem and the axion

2.1. Strong CP problem

The strong CP problem arises from the non-Abelian nature of the QCD gauge symmetry, or colour symmetry. Non-Abelian gauge potentials have disjoint sectors that cannot be transformed continuously into one another. Each of these vacuum configurations can be labelled by an integer, the topological winding number, n. Quantum tunnelling occurs between vacua. Consequently, the gauge invariant QCD vacuum state is a superposition of these states, i.e.,

$$|\theta\rangle = \sum_n e^{-in\theta}|n\rangle \ . \tag{1}$$

The angle, θ, is a parameter which describes the QCD vacuum state, $|\theta\rangle$.

In the massless quark limit, QCD possesses a classical chiral symmetry. However, this symmetry is not present in the full quantum theory due to the Adler-Bell-Jackiw anomaly [26, 27]. In the full quantum theory, including quark masses, the physics of QCD remains unchanged under the following transformations of the quark fields, q_i, quark masses, m_i, and vacuum parameter, θ:

$$q_i \ \rightarrow e^{i\alpha_i \gamma_5/2} q_i \tag{2}$$

$$m_i \rightarrow e^{-i\alpha_i} m_i \tag{3}$$

$$\theta \ \rightarrow \theta - \sum_{i=1}^{N} \alpha_i \ , \tag{4}$$

where the α_i are phases and γ_5 is the usual product of gamma matrices. This is not a symmetry of QCD due to the change in θ.

The transformations of Eq. (2) through Eq. (4) can be used to move phases between the quark masses and θ. However, the quantity,

$$\overline{\theta} \equiv \theta - \arg \det \mathcal{M} = \theta - \arg(m_1 m_2 ... m_N) , \qquad (5)$$

where $\mathcal{M}$ is the quark mass matrix, is invariant and thus observable, unlike θ.

The presence of θ in QCD violates the discrete symmetries P and CP. However, CP violation has not been observed in QCD. An electric dipole moment for the neutron is the most easily observed consequence of QCD, or strong, CP violation. θ results in a neutron electric dipole moment of [21, 22, 23, 24],

$$|d_n| \sim 10^{-16} \, \overline{\theta} \, e \, \text{cm} , \qquad (6)$$

where e is the electric charge. The current experimental limit is [28]

$$|d_n| < 6.3 \times 10^{-26} \, e \, \text{cm} \qquad (7)$$

and thus, $|\overline{\theta}| \lesssim 10^{-9}$. There is no natural reason to expect $\overline{\theta}$ to be this small. CP violation occurs in the standard model by allowing the quark masses to be complex and thus the natural value of θ is expected to be of order one. This is the strong CP problem, i.e. the question of why the angle $\overline{\theta}$ should be nearly zero, despite the presence of CP violation in the standard model.

The Peccei-Quinn (PQ) solution [1, 2] to this problem results in an axion [3, 4]. While other solutions to the strong CP problem have been proposed, the presence of the axion in the PQ solution makes it the most interesting when searching for the dark matter of the universe. Thus, we focus on this solution only in the following.

2.2. The Peccei-Quinn solution

The axion is the pseudo-Nambu-Goldstone boson from the Peccei-Quinn solution to the strong CP problem [1, 2, 3, 4]. In the PQ solution, $\overline{\theta}$ is promoted from a parameter to a dynamical variable. This variable relaxes to the minimum of its potential and hence is small.

To implement the PQ mechanism, a global symmetry, $U(1)_{PQ}$, is introduced. This symmetry possesses a colour anomaly and is spontaneously broken. The axion is the resulting Nambu-Goldstone boson and its field, a, can be redefined to absorb the parameter $\overline{\theta}$. While initially massless, non-perturbative effects, which make QCD $\overline{\theta}$ dependent, also result in a potential for the axion. This potential causes the axion to acquire a mass and relax to the CP conserving minimum, solving the strong CP problem.

As there are no degrees of freedom available for the axion in the standard model, new fields must be added to realize the PQ solution. In the original, Peccei-Quinn-Weinberg-Wilczek (PQWW) axion model, an extra Higgs doublet was used. We review this model to demonstrate the PQ mechanism.

Assume that one of the two Higgs doublets in the model, ϕ_u, couples to up-type quarks with strengths y_i^u and the other, ϕ_d, couples to down-type quarks with strengths y_i^d, where i gives the variety of up- or down-type quark. We label the up- and down-type quarks u_i and d_i, respectively (rather than q_i, as in the previous section). With a total of N quarks, there are $N/2$ up-type quarks and down-type quarks. The leptons may acquire mass via Yukawa couplings to either of the Higgs doublets or

to a third Higgs doublet. We ignore this complication here and simply examine the couplings to quarks.

The quarks acquire their masses from the expectation values of the neutral components of the Higgs, ϕ_u^0 and ϕ_d^0. The mass generating couplings are

$$\mathcal{L}_m = y_i^u u_{Li}^\dagger \phi_u^0 u_{Ri} + y_i^d d_{Li}^\dagger \phi_d^0 d_{Ri} + \text{h.c.} \ . \tag{8}$$

Peccei and Quinn chose the Higgs potential to be

$$V(\phi_u, \phi_d) = -\mu_u^2 \phi_u^\dagger \phi_u - \mu_d^2 \phi_d^\dagger \phi_d + \sum_{i,j} a_{ij} \phi_i^\dagger \phi_i \phi_j^\dagger \phi_j + \sum_{i,j} b_{ij} \phi_i^\dagger \phi_j \phi_j^\dagger \phi_i \ , \tag{9}$$

where the matrices (a_{ij}) and (b_{ij}) are real and symmetric and the sum is over the two types of Higgs fields. With this choice of potential, the full Lagrangian has a global $U_{PQ}(1)$ invariance,

$$\phi_u \rightarrow e^{i2\alpha_u} \phi_u \tag{10}$$

$$\phi_d \rightarrow e^{i2\alpha_d} \phi_d \tag{11}$$

$$u_i \rightarrow e^{-i\alpha_u \gamma_5} u_i \tag{12}$$

$$d_i \rightarrow e^{-i\alpha_d \gamma_5} d_i \tag{13}$$

$$\overline{\theta} \rightarrow \overline{\theta} - N(\alpha_u + \alpha_d) \ . \tag{14}$$

When the electroweak symmetry breaks, the neutral Higgs components acquire vacuum expectation values:

$$\langle \phi_u^0 \rangle = v_u e^{iP_u/v_u} \tag{15}$$

$$\langle \phi_d^0 \rangle = v_d e^{iP_d/v_d} \ . \tag{16}$$

One linear combination of the Nambu-Goldstone fields, P_u and P_d, is the longitudinal component of the Z-boson,

$$h = \cos\beta_v P_u - \sin\beta_v P_d \ . \tag{17}$$

The orthogonal combination is the axion field,

$$a = \sin\beta_v P_u + \cos\beta_v P_d \ . \tag{18}$$

Using Eqs. (15), (16), (17) and (18) with Eq. (8), the axion couplings to quarks arise from

$$-\mathcal{L}_m = m_i^u u_{Li}^\dagger e^{i\frac{\sin\beta_v}{v_u}a} u_{Ri} + m_i^d d_{Li}^\dagger e^{i\frac{\cos\beta_v}{v_d}a} d_{Ri} + \text{h.c.} \ , \tag{19}$$

where $m_i^u = y^{u_i} v_u$ and $m_i^d = y_i^d v_d$. The axion field dependence can be moved from the mass terms using the transformations of Eqs. (12), (13) and (14). Direct couplings between the axion and quarks will remain in the Lagrangian, through the quark kinetic term. Defining $v = \sqrt{v_u^2 + v_d^2}$, the corresponding change in $\overline{\theta}$ is

$$\overline{\theta} \rightarrow \overline{\theta} - N(v_u/v_d + v_d/v_u)a/v \ , \tag{20}$$

which can be absorbed by a redefinition of the axion field.

Non-perturbative QCD effects explicitly break the PQ symmetry, but do not become important until confinement occurs. These effects give the axion field a potential and when significant, the field relaxes to the CP conserving minimum. Hence the PQ mechanism, which replaces $\overline{\theta}$ with the dynamical axion field, solves the strong CP problem.

Under the PQWW scheme, the axion mass is tied to the electroweak symmetry breaking scale, resulting in a mass of the order of 100 keV. This heavy PQWW axion has been ruled out by observation, as discussed in Section 4.1. This does not, however, eliminate the possibility of solving the strong CP problem with an axion. In the following section, we discuss viable axion models.

2.3. Axion models

"Invisible" axion models, named so for their extremely weak couplings, are still possible. In an invisible axion model, the PQ symmetry is decoupled from the electroweak scale and is spontaneously broken at a much higher temperature, decreasing the axion mass and coupling strength. Two benchmark, invisible axion models exist: the Kim-Shifman-Vainshtein-Zakharov (KSVZ) [29, 30] and Dine-Fischler-Srednicki-Zhitnitsky (DFSZ) [31, 32] models. In both these models, an axion with permissable mass and couplings results.

In the KSVZ model, the only Higgs doublet is that of the standard model. The axion is introduced as the phase of an additional electroweak singlet scalar field. The known quarks cannot directly couple to such a field, as this would lead to unreasonably large quark masses. Instead, the scalar is coupled to an additional heavy quark, also an electroweak singlet. The axion couplings are then induced by the interactions of the heavy quark with the other fields.

The DFSZ model has two Higgs doublets, as in the PQWW model, and an additional electroweak singlet scalar. It is the electroweak singlet which acquires a vacuum expectation value at the PQ symmetry breaking scale. The scalar does not couple directly to quarks and leptons, but via its interactions with the two Higgs doublets.

PQ symmetries also occur naturally in string theory, via string compactifications, and are always broken by some type of instanton. While this could be expected to make the axion an outstanding dark matter candidate, string models favour a value of the PQ scale that is much higher than that allowed by cosmology (see the discussion in 3). A review of the current situation can be found in Ref. [33]. As discussed in [33], it is difficult to push the PQ scale far below 1.1×10^{16} GeV and easier to instead increase its value.

Generically, axion couplings to other particles are inversely proportional to f_a, however, the exact strength of these couplings are model dependent. For example, the coupling between axions and photons can be written,

$$\mathcal{L}_{a\gamma\gamma} = g_{a\gamma\gamma} a \mathbf{E} \cdot \mathbf{B} \ , \tag{21}$$

where $\mathbf{E}$ and $\mathbf{B}$ are the electromagnetic field components. The coupling constant is

$$g_{a\gamma\gamma} = \frac{g_\gamma \alpha}{\pi f_a} \ , \tag{22}$$

where α is the electromagnetic fine structure constant, 10^9 GeV $\lesssim f_a \lesssim 10^{12}$ GeV is the axion decay constant, of the order of the PQ scale, and g_γ is a constant containing the model dependence. Explicitly,

$$g_\gamma = \frac{1}{2} \left(\frac{E}{N} - \frac{2(4+z)}{3(1+z)} \right) \ , \tag{23}$$

where z is the ratio of the up and down quark masses, N is the axion colour anomaly and E, the axion electromagnetic anomaly [34]. The term containing the ratios of light quark masses is approximately equal to 1.95. The model dependence arises through the ratio, E/N. In grand-unifiable models, E and N are related and $E/N = 8/3$. The DFSZ axion model falls into this category and in this case, $g_\gamma = 0.36$. For a KSVZ axion, $E = 0$ and $g_\gamma = -0.97$.

It is possible for an axion to solve the strong CP problem, as shown by the existence of the KSVZ and DFSZ axion models. While significant for that alone, the axion also provides an interesting candidate for the cold dark matter of the universe.

3. Cosmological production of axions

3.1. Properties of axion dark matter

Axions satisfy the two criteria necessary for cold dark matter: (1) a non-relativistic population of axions could be present in our universe in sufficient quantities to provide the required dark matter energy density and (2) they are effectively collisionless, i.e., the only significant long-range interactions are gravitational.

Despite having a very small mass [21, 22, 23, 24],

$$m_a \simeq 6 \times 10^{-6} \text{ eV } \left(\frac{10^{12}\text{GeV}}{f_a} \right) , \tag{24}$$

axion dark matter is non-relativistic, as cold populations are produced out of equilibrium. There are three mechanisms via which cold axions are produced: vacuum realignment [5, 6, 7], string decay [8, 9, 10, 11, 12, 13, 14, 15, 16, 17, 18] and domain wall decay [18, 19, 20]. In this section, we discuss the history of the axion field as the universe expands and cools to see how and when axions are produced. We also review vacuum realignment production in detail, as there will always be a contribution to the cold axion populations from this mechanism and, as discussed below, it may provide the only contribution. A complete description of the cold axion populations can be found in ref. [35].

3.2. Topological axion production

There are two important scales in dark matter axion production. The first is the temperature at which the PQ symmetry breaks, T_{PQ}. Which of the three mechanisms contribute significantly to the cold axion population depends on whether this temperature is greater or less than the inflationary reheating temperature, T_R. The second scale is the temperature at which the axion mass, arising from non-perturbative QCD effects, becomes significant. At high temperatures, the QCD effects are not significant and the axion mass is negligible [36]. The axion mass becomes important at a critical time, t_1, when $m_a t_1 \sim 1$ [5, 6, 7]. The temperature of the universe at t_1 is $T_1 \simeq 1$ GeV.

The PQ symmetry is unbroken at early times and temperatures greater than T_{PQ}. At T_{PQ}, it breaks spontaneously and the axion field, proportional to the phase of the complex scalar field acquiring a vacuum expectation value, may have any value. The phase varies continuously, changing by order one from one horizon to the next. Axion strings appear as topological defects.

If $T_{PQ} > T_R$, the axion field is homogenized over vast distances and the string density is diluted by inflation, to a point where it is extremely unlikely that our visible universe contains any axion strings. In the case $T_{PQ} < T_R$, the axion field is not homogenized and strings radiate cold, massless axions until non-perturbative QCD effects become significant at temperature, T_1. Agreement has not been reached on the expected spectrum of axions from string radiation and there are two possibilities. Either strings oscillate many times before they completely decay and axion production is strongly peaked around a dominant mode [8, 9, 11, 12, 13, 14, 15, 16] or much more rapid decay occurs, producing a spectrum inversely proportional to momentum [10, 37]. Rapid decay produces ~ 70 times less axions than slow string decay, leading to different cosmological bounds on the axion mass (see section 4.2).

When the universe cools to T_1, the axion strings become the boundaries of N domain walls. For $N = 1$, the walls rapidly radiate cold axions and decay (domain wall decay). If $N > 1$, the domain wall problem occurs [38] because the vacuum is multiply degenerate and there is at least one domain wall per horizon. These walls will end up dominating the energy density and cause the universe to expand as $S \propto t^2$, where S is the scale factor. Although other solutions to the domain wall problem have been proposed [18], we assume here that $N = 1$ or $T_{PQ} > T_R$.

Thus, if $T_{PQ} < T_R$, string and wall decay contribute to the axion energy density. If $T_R < T_{PQ}$, and the axion string density is diluted by inflation, these mechanisms do not contribute significantly to the density of cold axions. Then, only vacuum realignment will contribute a significant amount.

3.3. Vacuum realignment mechanism

Cold axions will be produced by vacuum realignment, independent of T_R. Details of this method are discussed below, but the general mechanism is as follows. At T_{PQ}, the axion field amplitude may have any value. If $T_{PQ} > T_R$, homogenization will occur due to inflation and the axion field will be single valued over our visible universe. Non-perturbative QCD effects cause a potential for the axion field. When these effects become significant, the axion field will begin to oscillate in its potential. These oscillations do not decay and contribute to the local energy density as non-relativistic matter. Thus, a cold axion population results from vacuum realignment, regardless of the inflationary reheating temperature.

To illustrate vacuum realignment, consider a toy axion model with one complex scalar field, $\phi(x)$, in addition to the standard model fields. The potential for $\phi(x)$ in our toy model is

$$V(\phi) = \frac{\lambda}{4}(|\phi|^2 - v_a^2)^2 \ , \tag{25}$$

When the universe cools to $T_{PQ} \sim v_a$, ϕ acquires a vacuum expectation value,

$$\langle \phi \rangle = v_a \exp(i\theta(x)) \ . \tag{26}$$

The relationship between the axion field, $a(x)$, and $\theta(x)$ is

$$a(x) \equiv v_a \theta(x) \ . \tag{27}$$

The axion decay constant in this model is

$$f_a \equiv \frac{v_a}{N} \ . \tag{28}$$

For the following discussion, we set $N = 1$.

At $T \sim \Lambda$, where Λ is the confinement scale, non-perturbative QCD effects give the axion a mass. An effective potential,

$$\widetilde{V}(\theta) = m_a^2(T)f_a^2(1 - \cos\theta) \ , \tag{29}$$

is produced. The axion acquires mass, m_a, due to the curvature of the potential at the minimum. This mass is temperature, and thus time, dependent due to the temperature dependence of the potential [36].

In a Friedmann-Robertson-Walker universe, the equation of motion for θ is

$$\ddot{\theta} + 3H(t)\dot{\theta} - \frac{1}{S^2(t)}\nabla^2\theta + m_a^2(T(t))\sin(\theta) = 0 \ , \tag{30}$$

where $S(t)$ is the scale factor and $H(t)$, the Hubble constant, at time t. Near $\theta = 0$, $\sin(\theta) \simeq \theta$.

We now restrict the discussion to the zero momentum mode. This is the only mode with significant occupation when $T_{PQ} > T_R$, so the final energy density calculated will be for this case. When $T_R > T_{PQ}$, higher modes will also be occupied. For the zero momentum mode, neglecting spatial derivatives, the equation of motion reduces to

$$\ddot{\theta} + 3H(t)\dot{\theta} + m_a^2(t)\theta = 0 \ , \tag{31}$$

i.e., the field satisfies the equation for a damped harmonic oscillator with time-dependent parameters. At early times, the axion mass is insignificant and θ is approximately constant. When the universe cools to the critical temperature, T_1, which we define via

$$m_a(T_1(t_1))t_1 \equiv 1 \ , \tag{32}$$

the field will begin to oscillate in its potential [39]. Given the definition of the critical time, t_1, in Eq. (32) [35],

$$t_1 \simeq 2 \times 10^{-7}\text{s} \left(\frac{f_a}{10^{12}\text{GeV}} \right)^{1/3} \tag{33}$$

and

$$T_1 \simeq 1\text{GeV} \left(\frac{10^{12}\text{GeV}}{f_a} \right)^{1/6} \ . \tag{34}$$

The axion field can realign only as fast as causality permits, thus the momentum of a quantum of the axion field is

$$p_a(t_1) \sim \frac{1}{t_1} \sim 10^{-9}\text{eV} \tag{35}$$

for $f_a \simeq 10^{12}$ GeV, which corresponds to $m_a \simeq 6$ μeV, by Eq. (24). Thus, this population is non-relativistic or cold.

The energy density of the scalar field around its potential minimum is

$$\rho = \frac{f_a^2}{2}[\dot{\theta}^2 + m_a^2(t)\theta^2] \ . \tag{36}$$

By the Virial theorem,

$$\langle\dot{\theta}^2\rangle = m_a^2\langle\theta^2\rangle = \frac{\rho}{f_a^2} \ . \tag{37}$$

As axions are non-relativistic and decoupled,

$$\rho \propto \frac{m_a(t)}{S^3(t)} \ . \tag{38}$$

Thus, the number of axions per comoving volume is conserved, provided the axion mass varies adiabatically.

The initial energy density of the coherent oscillations is

$$\rho_1 = \frac{1}{2} f_a^2 m_a^2(t_1)\theta_1^2 \tag{39}$$

and θ_1 is the initial, "misalignment" angle. The energy density in axions today is

$$\rho_0 = \rho_1 \frac{m_a(t_0)}{m_a(t_1)} \frac{S^3(t_1)}{S^3(t_0)} \ . \tag{40}$$

Using Eqs. (32) and (39),

$$\rho_0 = \frac{1}{2}f_a^2 \frac{m_a}{t_1}\left(\frac{S(t_1)}{S(t_0)}\right)^3 \theta_1^2 \, , \tag{41}$$

which implies the axion energy density,

$$\Omega_a \simeq 0.15 \left(\frac{f_a}{10^{12}\text{GeV}}\right)^{\frac{7}{6}} \theta_1^2 \, , \tag{42}$$

using Eqs. (24), (33) and (34).

As the axion couplings are very small, these coherent oscillations do not decay and make axions a good candidate for the dark matter of the universe.

4. Constraints on the axion

4.1. Laboratory bounds

The original PQWW axion would have been of order 100 keV mass, and possessed couplings large enough to enable the axion to have been produced and detected in conventional laboratory experiments. These included searches for axions emitted from reactors, where axions would compete with M1 gamma transitions in radioactive decay; nuclear deexcitation experiments; beam-dump experiments; and axion decay from 1^- heavy quarkonia states, i.e. J/ψ and Υ. All results were negative, thus excluding the original PQWW axion within a decade of its prediction. As these limits are much weaker than the current astrophysical upper bounds for both the mass and coupling to radiation, the reader is directed to earlier reviews [21, 22, 34], and the Particle Data Group Review of Particle Properties for discussion and annotated limits [40].

Searches for axions have also been performed exploiting the coherent mixing of axions with photons in experiments realized with lasers and large superconducting dipole magnets. These include both searches for vacuum dichroism and birefringence through the production of real or virtual axions in a magnetic field [41], and photon regeneration (shining light through walls) [42, 43, 44]. Axion-photon mixing will be discussed briefly further on, but the all such experiments to date have set limits on the axion-photon coupling, $g_{a\gamma\gamma} \sim 2 \times 10^{-7}$ GeV^{-1} (weakening significantly for $m_a > 0.5$ meV) orders of magnitude weaker than current astrophysical limits and direct searches for solar axions. While there are no prospects for the polarization experiments to compete with these latter ($g_{a\gamma\gamma} \sim 10^{-10}$ GeV^{-1}), a new strategy to resonantly-enhance photon regeneration may enable them to improve on these limits by up to an order of magnitude [45], and at least one such experiment is in preparation.

Torsion-balance techniques have enabled searches for axions through their coupling to the nucleon spin, and rigorous bounds have been set on their short-range interactions for masses below 1 meV. While impressive tour de force experiments, how to relate these limits to expectations from the Peccei-Quinn axion is not straightforward [46].

4.2. Cosmological bounds

Whether by the vacuum realignment mechanism, or by radiation from topological strings, the production of very light axions in the early universe implies an increasing energy density of the universe in axions for lower masses: $\Omega_a = \rho_a/\rho_c \propto m_a^{-7/6}$. As

the relative importance of the mechanisms is still controverted, a reliable lower bound on the axion mass should obtain where the vacuum realignment contribution becomes of order unity, $\Omega_a = \mathcal{O}(1)$. From Eq. (42), this corresponds to $m_a \sim 6\ \mu$eV(see section 3.3), although there is uncertainty in this estimate itself, owing to lack of knowledge of the initial value of θ within our horizon; the estimate above based on the assumption that this parameter is of order unity. An accidentally small value would drive the mass associated with closure density downwards, including arbitrarily small masses. On the other hand, within the concordance model, $\Omega_{DM} = 0.23$, implying that the axion mass should be roughly a factor of 4 higher than cited above. Thus the ADMX microwave cavity experiment conservatively began its search campaign at $m_a \sim 2\ \mu$eV, and continues to work upwards. Recent discussions of the cosmological bound from vacuum realignment can be found in refs. [47, 48].

The above vacuum realignment bound applies when inflation has homogenized the axion field over our horizon. When the PQ scale breaks after inflation, cold axions are additionally produced by string and domain wall decay. These extra contributions mean that we require inflation to have produced less axions to avoid overclosing the universe and thus, the axion mass lower bound increases (see section 3.3). As the spectrum of axions from string radiation is debated, we review the possible bounds. If axion strings decay rapidly, giving a spectrum inversely proportional to momentum, the lower bound for the axion mass is $\sim 15\ \mu$eV [17]. If the decay is less rapid and strings go through many oscillations, an analysis based on local strings [15] gives a lower bound of $100\ \mu$eV. A similar analysis based on global strings [16] gives a smaller lower bound of $30\ \mu$eV. Given that the PQ symmetry is global, it is likely that the lower bound of $30\ \mu$eV is applicable if the PQ symmetry breaks after inflation and axion strings decay slowly.

4.3. Astrophysical bounds

In general, introducing a channel for direct or free-streaming energy loss from a star's core accelerates the star's evolution. The core will contract and heat up under the influence of gravity when axions (or other exotica) compete with the production of strongly trapped photons, whose radiation pressure acts to counterbalance gravitational pressure. Furthermore, for each stellar system, axions are excluded only over a finite range of couplings. As the axion's coupling is increased in the stellar-evolution simulations, the free-streaming lower limit of the axion's excluded couplings is reached at a point where deviations from an axion-free model first become noticeable. However, as the coupling is further increased, the axions themselves eventually become strongly trapped; the upper limit corresponds to the regime where their influence on evolution diminishes below the threshold of observation. A comprehensive treatment of such constraints on properties of axions and other exotica has been published by Raffelt [49]. The two most relevant astrophysical limits in framing the region of interest where axions may be the dark matter are described below.

The most stringent constraint on the axion-photon coupling presently is due to horizontal branch (HB) stars, i.e. those that are in their helium-burning phase, within globular clusters. Globular clusters provide a cohort population of stars of all the same age; those that are seen today are have masses somewhat less than that of our sun. By the ratio of the number observed in the HB phase to those in the red giant phase, i.e. after exhaustion of core-hydrogen burning but before the helium flash, one statistically infers an average HB lifetime. The concordance (within 10%)

between the calculated and inferred HB lifetime precludes Primakoff production of axions ($\gamma + Ze \rightarrow a + Ze$, i.e. axions produced by the interaction of a real plus virtual photon) at a level corresponding to an upper bound of $g_{a\gamma\gamma} < 10^{-10}$ GeV^{-1}. A definitive study of axion cooling in stars using numerical methods aims to extend this analysis [50].

The lowest-lying upper bound for the axions mass is due to SN1987a. Axions produced by nucleon-nucleon bremsstrahlung ($N + N \rightarrow N + N + a$) during the core-bounce of the protoneutron star would have competed with neutrino emission. That the duration of the neutrino pulse observed between the IMB and Kamioka water Cherenkov detectors (19 events over 10 seconds) was in good accord with core-collapse models precludes axions in the mass range 10^{-3} eV $< m_a < 2$ eV. This range corresponds to the free-streaming regime; as mentioned previously, for axions above this range axions themselves are strongly trapped and thus are not effective in quenching the neutrino signal.

5. Phase-space structure of halo dark matter

The local velocity distribution of dark matter axions is of vital importance for direct detection. The Axion Dark Matter eXperiment (ADMX), detailed in Section 6.2 and ref. [51], in this volume, uses a microwave cavity to search directly for axions. The observed signal is the power output from the cavity due to axion conversion to photons, as a function of frequency. The frequency corresponds to the energy distribution of axions undergoing conversion. As axions are non-relativistic, the signal frequency is given by:

$$\nu(v) = \frac{m_a}{h}\left(c^2 + \frac{1}{2}v^2\right) \ . \tag{43}$$

The local velocity distribution thus determines the signal shape. The signal amplitude is determined by the density of axions of a particular energy. Thus, the phase-space distribution determines the signal observed.

We expect that the dark halo of the Milky Way consists of a number of components which ADMX is capable of observing: (1) a thermalized component with a Maxwell-Boltzmann velocity distribution, (2) discrete flows, from tidal stripping of satellite halos or coherent dark matter flows crossing the halo, and (3) overdense regions that are not gravitationally bound, known as caustics.

The ADMX search technique assumes that the rates of change of velocity, velocity dispersion and flow density are slow compared to the time scale of the experiment. The ADMX medium resolution (MR) channel searches for an isothermal component of the halo as dark matter axions. The ADMX high resolution (HR) channel searches for signals with a narrow velocity dispersion, such as discrete flows.

Numerical simulations produce large halos within which hundreds of smaller clumps, or subhalos, exist [52, 53]. Tidal disruption of these subhalos leads to flows in the form of "tidal tails" or "streams." The Earth may currently be in a stream of dark matter from the Sagittarius A dwarf galaxy [54, 55]. This stream of subhalo debris satisfies both the requirements of small velocity dispersion and a repeatable signal and thus may be detectable by the ADMX HR channel.

Non-thermalized flows from late infall of dark matter onto the halo have also been shown to be expected [56, 57]. The idea behind these flows is that dark matter that has only recently fallen into the gravitational potential of the galaxy will have had

insufficient time to thermalize with the rest of the halo and will be present in the form of discrete flows. There will be one flow of particles falling onto the galaxy for the first time, one due to particles falling out of the galaxy's gravitational potential for the first time, one from particles falling into the potential for the second time, etc. Furthermore, where the gradient of the particle velocity diverges, particles "pile up" and form caustics. In the limit of zero flow velocity dispersion, caustics have infinite particle density. The velocity dispersion of cold axions at a time, t, prior to galaxy formation is approximately $\delta v_a \sim 3 \times 10^{-17}(10^{-5}\text{eV}/m_a)(t_0/t)^{2/3}$ [58], where t_0 is the present age of the universe. A flow of dark matter axions will thus have a small velocity dispersion, leading to a large, but finite density at a caustic.

The caustic ring model, under the assumptions of self-similarity and axial symmetry, predicts that the Earth is located near a caustic feature [59]. This model, fitted to rises in the Milky Way rotation curve and a triangular feature seen in the IRAS maps, predicts that the flows falling in and out of the halo for the fifth time contain a significant fraction of the local halo density. The predicted densities are 1.5×10^{-24} g/cm^3 and 1.5×10^{-25} g/cm^3 [60], comparable to the local dark matter density of 9.2×10^{-25} g/cm^3 predicted by Gates et al. [61]. The flow of the greatest density is known as the "Big Flow."

A general treatment of the phase-space structure of dark matter halos, which does not require assumptions of self-similarity or symmetry, has recently been developed [62]. This treatment studies the statistics of dark matter caustics in the tidal debris remaining from mergers of smaller halos to form galaxies and from the primordial coldness of dark matter. While more general than the approach of ref. [60], this treatment only results in a statistical distribution and does not give specific predictions for our galactic halo.

Additionally, numerical methods have been developed to study caustics and flows in dark matter halos. To date, most numerical simulations are too coarse-grained to resolve caustic structure, although its presence can be observed when special techniques are used [63, 64, 65, 66, 67]. The recent work of ref. [68] predicts at least 10^5 discrete streams near our Sun, although specific predictions are not made for the stream densities and velocities.

It has also recently been shown that dark matter axions can exist in the form of a Bose-Einstein condensate (BEC)[69]. If this is the case, the formation of caustics is suppressed within the BEC. However, vortices are expected to form at the center of galactic halos, due to their net rotation. Within a vortex, axion dark matter will exist in the normal phase and flows and caustics will still be present.

The possible existence of discrete flows provides an opportunity to increase the discovery potential of ADMX. A discrete axion flow produces a narrow peak in the spectrum of microwave photons in the experiment and such a peak can be searched for with higher signal-to-noise than the signal from axions in an isothermal halo. If such a signal is found, it will provide detailed information on the structure of the Milky Way halo.

6. Experimental searches for dark-matter axions

6.1. Axion-photon mixing

As pseudoscalars, axions can be produced by the interaction of two photons, one of which can be virtual, $\gamma + \gamma* \to a$, the process being known as the Primakoff

effect [70]. This implies that photons and axions may mix in the presence of an external electromagnetic field, through the Lagrangian density of Eq. (21). In all axion searches based on the Primakoff effect to date, $\mathbf{E}$ represents the electric field of the real photon, and $\mathbf{B}$ is an external magnetic field. Although the opposite combination is possible, it is vastly easier to produce and support a static magnetic field than the equivalent electric field; a 1 T magnetic field being equal to an electric field of 30 MV/cm in gaussian units. In fact, fields of order 10 T are readily achieved today with superconducting magnets. The coherent mixing of axions and photons within magnetic fields of large spatial extent enables searches of exceedingly high sensitivity, although there is yet no experimental strategy capable of reaching the standard Peccei-Quinn axion over the entire open range.

A general formulism for axion-photon mixing in external magnetic fields, including plasma effects, is found in Ref. [71].

6.2. The microwave cavity experiment for dark-matter axions

In 1983, Sikivie proposed two independent schemes to detect the axion based on the Primakoff effect [72, 73]. The first was a search for axions constituting halo dark matter by their resonant conversion to RF photons in a microwave cavity permeated by a strong magnetic field. Tuning the cavity to fulfill the resonant condition, $h\nu = m_a c^2 (1 + \mathcal{O}(\beta^2 \sim 10^{-6}))$, and assuming axions saturate the galactic halo, the conversion power from an optimized experiment is given by:

$$P = g_{a\gamma\gamma}^2 \frac{V B^2 \rho_a Q}{m_a}, \tag{44}$$

where B is the strength of the magnetic field, V the cavity volume and Q is the cavity quality factor. The most sensitive microwave cavity experiment (and in fact the only one currently in operation) is ADMX at Lawrence Livermore National Laboratory. This search has excluded axions of KSVZ axion-photon coupling as the local halo dark matter, for a narrow range of masses $1.9 < m_a < 3.4$ μeV.

The anticipated conversion power is miniscule, even for the largest superconducting magnets feasible; for ADMX the signal expected is of order 10^{-22} watts. Furthermore, as the experiment will necessitate tuning orders of magnitude of frequency in small frequency steps, there are limits on how long one may integrate at each frequency to improve the signal-to-noise, as governed by the Dicke radiometer equation [74]:

$$\frac{s}{n} \equiv \frac{P_s}{P_n} = \frac{P_s \sqrt{\Delta\nu t}}{k T_n} \ . \tag{45}$$

Here s/n is the signal-to-noise ratio, $\Delta\nu$ the bandwidth of the signal, t the integration time, and P_s and P_n the signal and noise power respectively. This puts a clear premium on reducing the total system noise temperature, which is the sum of the physical temperature and the equivalent electronic noise temperature of the amplifier, $T_n = T_{phys} + T_{elec}$. ADMX has recently completed an upgrade from conventional heterojunction field-effect transistors (HFETs, or HEMTs) with an noise equivalent temperature of $T_{elec} \sim 2$ K, to SQUID amplifiers, whose noise equivalent noise temperatures can reach the quantum limit, $T_{elec} \sim 50$ mK at 750 MHz when cooled to comparable physical temperatures. This strategy will enable them ultimately to reach the DFSZ model axions, as well as cover the open mass range much faster. The microwave cavity experiments is described by Carosi elsewhere in this volume [51].

6.3. Other current axion searches

In the same report, Sikivie also outlined how to detect axions free-streaming from the Sun's nuclear burning core [72, 73]. Axion production would be dominated by the Primakoff process $\gamma + Ze \rightarrow a + Ze$; for KSVZ axions, the integrated solar flux at the Earth would be given by $F_a = 7.4 \times 10^{11} m_a^2 [\text{eV}] \text{ cm}^{-2}\text{s}^{-1}$, emitted with a thermal spectrum of mean energy ~ 4.2 keV. For relativistic axions, the conversion probability to photons of the same energy in a uniform magnetic field is given by $P(a \rightarrow \gamma) = \Pi = (1/4)(g_{a\gamma\gamma}BL)^2|F(q)|^2$, where B is the strength of the magnetic field, and L its length‡. $F(q) \equiv \int dx e^{iqx} B(x)/B_0 L$ represents the form-factor of the magnetic field with respect to the momentum mismatch between the massive axion and massless photon of the same energy, $q = k_a - k_\gamma = (\omega^2 - m_a^2)^{1/2} - \omega \sim m_a^2/2\omega$. $|F(q)|$ is unity in the limit $ql << 2\pi$, but oscillates and falls off rapidly for $ql > 2\pi$, where the axions are no longer sufficiently relativistic to stay in phase with the photon for maximum mixing.

Utilizing a prototype LHC dipole magnet as the basis for its axion helioscope, the CAST collaboration have recently published the best limits on the solar axions, $g_{a\gamma\gamma} < 0.88 \times 10^{-10}$ GeV^{-1}, valid for $m_a < 10^{-2}$ eV [75], slightly more stringent than those derived from horizontal branch stars. This collaboration has also pushed the sensitivity of the search upward in mass into the region of axion models, by introducing a gas (^{4}He) of variable pressure into the magnet bore. In this case, the plasma frequency $\omega_p = (4\pi\alpha N_e/m_e)^{1/2} \equiv m_\gamma$ endows the x-ray photon with an effective mass; thus full coherence of the axion and photon states can be restored, and the theoretical maximum conversion probability achieved for any axion mass, by the filling the magnet with a gas of the appropriate density [76]. The mass range can thereby be extended upwards in scanning mode, by tuning the gas pressure in small steps to as high as feasible. In this manner, axions have now been excluded part-way into the Peccei-Quinn model band, $g_{a\gamma\gamma} < 2.2 \times 10^{-10}$ GeV^{-1} (95% c.l.), valid for $m_a < 0.4$ eV [77]. This phase of the experiment continues with ^{3}He gas which will permit probing of yet higher masses; for further details, see Zioutas elsewhere in this volume [78].

Purely laboratory bounds on axions or generalized pseudoscalars have also been established without relying on either astrophysical or cosmological sources. In photon regeneration ("shining light through walls") axions are coherently produced by shining a laser beam through a transverse dipole magnet, and reconverted to real photons in a colinear dipole magnet on the other side of an optical barrier [79, 80]. The probability to detect a photon per laser photon is given by $P(a \rightarrow \gamma \rightarrow a) = \Pi^2$. While current limits from photon regeneration ($g_{a\gamma\gamma} < 2 \times 10^{-7}$ GeV^{-1}, $m_a < 0.5 \times 10^{-3}$ eV) [42, 43, 44] have not so far been competitive with solar searches, the scheme may be resonantly enhanced utilizing actively locked Fabry-Perot optical cavities to strengthen limits potentially by an order of magnitude beyond those of CAST and Horizontal Branch stars [45].

7. Summary

The current state of the standard QCD axion is shown in Figure 1 [40]. While it represents an oversimplification of the situation, insofar as the various experimental

---

‡ A useful mnemonic in rate estimates for experiments is that, within a few percent, the factor $(g_{10}B_{10}L_{10})^2 \approx 10^{-16}$, where $g_{10} \equiv 10^{-10}$ GeV^{-1}, $B_{10} \equiv 10$ T, and $L_{10} \equiv 10$ m.
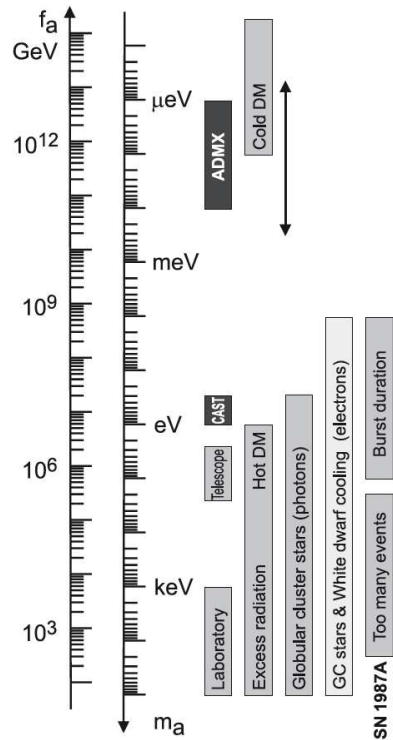
Figure 1. Constraints on the PQ-scale f_a and corresponding m_a from astrophysics, cosmology and laboratory experiments. The light grey regions are most model-dependent. From ref. [40].

and observational limits on mass are model-dependent, the central point is that there is a substantial window for axionic dark matter, and that the upgraded ADMX will be able to cover about two of the three decades in mass. One should be open to surprise from experiments such as CAST which are looking in regions of mass and coupling constant where axions are not expected to be the dark matter, but could find axion-like pseudoscalars associated with our first forays into beyond-Standard Model phenomenology.

Acknowledgments

References

[1] R. D. Peccei and H. R. Quinn. CP Conservation in the Presence of Instantons. *Phys. Rev. Lett.*, 38:1440–1443, 1977.

[2] R. D. Peccei and H. R. Quinn. Constraints Imposed by CP Conservation in the Presence of Instantons. *Phys. Rev.*, D16:1791–1797, 1977.

[3] S. Weinberg. A New Light Boson? *Phys. Rev. Lett.*, 40:223–226, 1978.

[4] F. Wilczek. Problem of Strong P and T Invariance in the Presence of Instantons. *Phys. Rev. Lett.*, 40:279–282, 1978.

[5] L. F. Abbott and P. Sikivie. A Cosmological Bound on the Invisible Axion. *Phys. Lett.*, B120:133–136, 1983.

[6] J. Preskill, M. B. Wise, and F. Wilczek. Cosmology of the Invisible Axion. *Phys. Lett.*, B120:127–132, 1983.

[7] M. Dine and W. Fischler. The Not-So-Harmless Axion. *Phys. Lett.*, B120:137–141, 1983.

[8] R. L. Davis. Goldstone Bosons in String Models of Galaxy Formation. *Phys. Rev.*, D32:3172, 1985.

[9] R. L. Davis. Cosmic Axions From Cosmic Strings. *Phys. Lett.*, B180:225, 1986.

[10] D. Harari and P. Sikivie. On the Evolution of Global Strings in the Early Universe. *Phys. Lett.*, B195:361, 1987.

[11] A. Vilenkin and T. Vachaspati. Radiation of Goldstone Bosons from Cosmic Strings. *Phys. Rev.*, D35:1138, 1987.

[12] R. L. Davis and E. P. S. Shellard. Do Axions Need Inflation? *Nucl. Phys.*, B324:167, 1989.

[13] A. Dabholkar and J. M. Quashnock. Pinning Down the Axion. *Nucl. Phys.*, B333:815, 1990.

[14] R. A. Battye and E. P. S. Shellard. Global String Radiation. *Nucl. Phys.*, B423:260–304, 1994.

[15] R. A. Battye and E. P. S. Shellard. Axion String Constraints. *Phys. Rev. Lett.*, 73:2954–2957, 1994.

[16] M. Yamaguchi, M. Kawasaki, and J. Yokoyama. Evolution of Axionic Strings and Spectrum of Axions Radiated From Them. *Phys. Rev. Lett.*, 82:4578–4581, 1999.

[17] C. Hagmann, S. Chang, and P. Sikivie. Axion Radiation from Strings. *Phys. Rev.*, D63:125018, 2001.

[18] S. Chang, C. Hagmann, and P. Sikivie. Studies of the Motion and Decay of Axion Walls Bounded by Strings. *Phys. Rev.*, D59:023505, 1999.

[19] D. H. Lyth. Estimates of the Cosmological Axion Density. *Phys. Lett.*, B275:279–283, 1992.

[20] M. Nagasawa and M. Kawasaki. Collapse of Axionic Domain Wall and Axion Emission. *Phys. Rev.*, D50:4821–4826, 1994.

[21] J. E. Kim. Light Pseudoscalars, Particle Physics and Cosmology. *Phys. Rept.*, 150:1–177, 1987.

[22] H.-Y. Cheng. The Strong CP Problem Revisited. *Phys. Rept.*, 158:1, 1988.

[23] M. S. Turner. Windows on the Axion. *Phys. Rept.*, 197:67–97, 1990.

[24] G. G. Raffelt. Astrophysical Methods to Constrain Axions and Other Novel Particle Phenomena. *Phys. Rept.*, 198:1–113, 1990.

[25] Jihn E. Kim and Gianpaolo Carosi. Axions and the Strong CP Problem. *[arXiv:0807.3125]*, 2008.

[26] S. L. Adler. Axial Vector Vertex in Spinor Electrodynamics. *Phys. Rev.*, 177:2426–2438, 1969.

[27] J. S. Bell and R. Jackiw. A PCAC Puzzle: $pi^0 \rightarrow \gamma\gamma$ in the Sigma Model. *Nuovo Cim.*, A60:47–61, 1969.

[28] P. G. Harris, C. A. Baker, K. Green, P. Iaydijiev, S. Ivanov, D. J. R. May, J. M. Pendlebury, D. Shiers, K. F. Smith, M. van der Grinten, and P. Geltenbort. New Experimental Limit on the Electric Dipole Moment of the Neutron. *Phys. Rev. Lett.*, 82:904–907, 1999.

[29] J. E. Kim. Weak Interaction Singlet and Strong CP Invariance. *Phys. Rev. Lett.*, 43:103, 1979.

[30] M. A. Shifman, A. I. Vainshtein, and V. I. Zakharov. Can Confinement Ensure Natural CP Invariance of Strong Interactions? *Nucl. Phys.*, B166:493, 1980.

[31] M. Dine, W. Fischler, and M. Srednicki. A Simple Solution to the Strong CP Problem with a Harmless Axion. *Phys. Lett.*, B104:199, 1981.

[32] A. R. Zhitnitsky. On Possible Suppression of the Axion Hadron Interactions. (in Russian). *Sov. J. Nucl. Phys.*, 31:260, 1980.

[33] Peter Svrček and Edward Witten. Axions in string theory. *JHEP*, 06:051, 2006.

[34] L. J. Rosenberg and K. A. van Bibber. Searches for invisible axions. *Phys. Rept.*, 325:1–39, 2000.

[35] Pierre Sikivie. Axion cosmology. *Lect. Notes Phys.*, 741:19–50, 2008.

[36] D. J. Gross, R. D. Pisarski, and L. G. Yaffe. QCD and Instantons at Finite Temperature. *Rev. Mod. Phys.*, 53:43, 1981.

[37] C. Hagmann and P. Sikivie. Computer simulations of the motion and decay of global strings. *Nucl. Phys.*, B363:247–280, 1991.

[38] P. Sikivie. Of Axions, Domain Walls and the Early Universe. *Phys. Rev. Lett.*, 48:1156, 1982.

[39] E. W. Kolb and M. S. Turner. *The Early Universe*. Addison-Wesley Publishing Company, Reading, MA, 1994.

[40] C. Amsler et al. Review of particle physics. *Phys. Lett.*, B667:1, 2008.

[41] Y. Semertzidis et al. Limits on the production of light scalar and pseudoscalar particles. *Phys. Rev. Lett.*, 64:2988–2991, 1990.

[42] R. Cameron et al. Search for nearly massless, weakly coupled particles by optical techniques. *Phys. Rev.*, D47:3707–3725, 1993.

[43] Cecile Robilliard et al. No light shining through a wall. *Phys. Rev. Lett.*, 99:190403, 2007.

[44] Aaron S. Chou et al. Search for axion-like particles using a variable baseline photon regeneration technique. *Phys. Rev. Lett.*, 100:080402, 2008.

[45] P. Sikivie, D. B. Tanner, and Karl van Bibber. Resonantly enhanced axion - photon regeneration. *Phys. Rev. Lett.*, 98:172002, 2007.

[46] E. G. Adelberger, J. H. Gundlach, B. R. Heckel, S. Hoedl, and S. Schlamminger. Torsion balance experiments: A low-energy frontier of particle physics. *Prog. Part. Nucl. Phys.*, 62:102–134, 2009.

[47] Mark P Hertzberg, Max Tegmark, and Frank Wilczek. Axion Cosmology and the Energy Scale of Inflation. *Phys. Rev.*, D78:083507, 2008.

[48] Luca Visinelli and Paolo Gondolo. Dark Matter Axions Revisited. *[arXiv:0903.4377]*, 2009.

[49] G. G. Raffelt. *Stars as laboratories for fundamental physics: The astrophysics of neutrinos, axions, and other weakly interacting particles.* University Press, Chicago, USA, 1996.

[50] L. D. et al. Duffy. Axion cooling in massive stars. *in prep.*, 2009.

[51] G. Carosi. Axion searches: ADMX. *New Journal of Physics*, 2009.

[52] J. F. Navarro, C. S. Frenk, and S. D. M. White. The Structure of Cold Dark Matter Halos. *Astrophys. J.*, 462:563–575, 1996.

[53] B. Moore, F. Governato, T. Quinn, J. Stadel, and G. Lake. Resolving the Structure of Cold Dark Matter Halos. *Astrophys. J.*, 499:L5, 1998.

[54] K. Freese, P. Gondolo, H. J. Newberg, and M. Lewis. The Effects of the Sagittarius Dwarf Tidal Stream on Dark Matter Detectors. *Phys. Rev. Lett.*, 92:111301, 2004.

[55] K. Freese, P. Gondolo, and H. J. Newberg. Detectability of Weakly Interacting Massive Particles in the Sagittarius Dwarf Tidal Stream. *Phys. Rev.*, D71:043516, 2005.

[56] P. Sikivie and J. R. Ipser. Phase Space Structure of Cold Dark Matter Halos. *Phys. Lett.*, B291:288–292, 1992.

[57] A. Natarajan and P. Sikivie. The Inner Caustics of Cold Dark Matter Halos. *Phys. Rev.*, D73:023510, 2006.

[58] P. Sikivie. The Caustic Ring Singularity. *Phys. Rev.*, D60:063501, 1999.

[59] P. Sikivie. Evidence for Ring Caustics in the Milky Way. *Phys. Lett.*, B567:1–8, 2003.

[60] L. D. Duffy and P. Sikivie. The Caustic Ring Model of the Milky Way Halo. *Phys. Rev.*, D78:063508, 2008.

[61] E. I. Gates, G. Gyuk, and M. S. Turner. The Local Halo Density. *Astrophys. J.*, 449:L123–L126, 1995.

[62] Niayesh Afshordi, Roya Mohayaee, and Edmund Bertschinger. Hierarchical Phase Space Structure of Dark Matter Haloes: Tidal debris, Caustics, and Dark Matter annihilation. *[arXiv:0811.1582]*, 2008.

[63] A. G. Doroshkevich, E. V. Kotok, A. N. Poliudov, S. F. Shandarin, Iu. S. Sigov, and I. D. Novikov. Two-dimensional simulation of the gravitational system dynamics and formation of the large-scale structure of the universe. *Mon. Not. Roy. Astron. Soc.*, 192:321, 1980.

[64] A. A. Klypin and S. F. Shandarin. Three-dimensional numerical model of the formation of large-scale structure in the Universe. *Mon. Not. Roy. Astron. Soc.*, 204:891, 1983.

[65] J. Centrella and A. L. Melott. Three-dimensional simulation of large-scale structure in the universe. *Nature*, 305:196, 1983.

[66] A. L. Melott and S. F. Shandarin. Generation of large-scale cosmological structures by gravitational clustering. *Nature*, 346:633, 1990.

[67] David Stiff and Lawrence M. Widrow. Fine Structure of Dark Matter Halos and its Effect on Terrestrial Detection Experiments. *Phys. Rev. Lett.*, 90:211301, 2003.

[68] Mark Vogelsberger, Simon D. M. White, Amina Helmi, and Volker Springel. The fine-grained phase-space structure of Cold Dark Matter halos. *[arXiv:0711.1105]*, 2007.

[69] P. Sikivie and Q. Yang. Bose-Einstein Condensation of Dark Matter Axions. *[arXiv:0901.1106]*, 2009.

[70] H. Primakoff. Photo-Production of Neutral Mesons in Nuclear Electric Fields and the Mean Life of the Neutral Meson. *Phys. Rev.*, 81:899, 1951.

[71] Georg Raffelt and Leo Stodolsky. Mixing of the Photon with Low Mass Particles. *Phys. Rev.*, D37:1237, 1988.

[72] P. Sikivie. Experimental Tests of the "Invisible" Axion. *Phys. Rev. Lett.*, 51:1415, 1983.

[73] P. Sikivie. Detection rates for 'invisible' axion searches. *Phys. Rev.*, D32:2988, 1985.

[74] R.H. Dicke. The Measurement of Thermal Radiation at Microwave Frequencies. *Rev. Sci. Instrum.*, 17:268, 1946.

[75] S. Andriamonje et al. An improved limit on the axion-photon coupling from the CAST experiment. *JCAP*, 0704:010, 2007.

[76] K. van Bibber, P. M. McIntyre, D. E. Morris, and G. G. Raffelt. A practical laboratory detector for solar axions. *Phys. Rev.*, D39:2089, 1989.

[77] E. Arik et al. Probing eV-scale axions with CAST. *JCAP*, 0902:008, 2009.

[78] K. Zioutas. Axion searches with helioscopes and astrophysical signatures for axion(-like) particles. *New Journal of Physics*, 2009.

[79] K. Van Bibber, N. R. Dagdeviren, S. E. Koonin, A. Kerman, and H. N. Nelson. Proposed experiment to produce and detect light pseudoscalars. *Phys. Rev. Lett.*, 59:759–762, 1987.

[80] A. A. Anselm. Arion ↔ photon oscillations in a steady magnetic field (in Russian). *Yad. Fiz.*, 42:1480–1483, 1985.